Summer 6-1-1952

Plenoaste Crystals from an Olivian Basalt, Caballo Mountains, New Mexico

Charles Maxwell

Recommended Citation

Maxwell, Charles. "Plenoaste Crystals from an Olivian Basalt, Caballo Mountains, New Mexico." (1952). https://digitalrepository.unm.edu/eps_etds/184

Maxwell — Pleonaste Crystals from an Olivine Basalt

This thesis by Charles Maxwell
has been used by the following persons, whose signatures attest their acceptance of the above restrictions.

A Library which borrows this thesis for use by its patrons is expected to secure the signature of each user.

NAME AND ADDRESS	DATE
Petr. Research Corp. Geol. Dept. U of Colo.	11/4/68
[illegible] SW Expl Assoc	4/24/78
Anita Keller	11/20/82

Pleonaste Crystals from an Olivine Basalt,
Caballo Mountains, New Mexico.

by Charles Maxwell

A thesis
in partial fulfillment
of the requirements
for the Degree of
Master of Science
in Geology

The University of New Mexico
1952

This thesis, directed and approved by the candidate's committee, has been accepted by the Graduate Committee of the University of New Mexico in partial fulfillment of the requirements for the degree of

MASTER OF SCIENCE

E F Castetter
DEAN

6/2/52
DATE

Thesis committee

Carl W. Beck
CHAIRMAN

V. C. Kelley

J. Paul Fitzsimmons

CONTENTS

	Page
TABLES	ii
PLATES	iii
INTRODUCTION	1
Location and Accessibility	1
Physiography	1
Discovery and Utilization	2
Methods of Study	3
Acknowledgments	3
GENERAL GEOLOGY	4
PETROGRAPHY OF THE FLOW ROCKS	9
MINERALOGY OF PLEONASTE	21
Crystallography	21
Physical Properties	21
Structural Crystallography	30
X-ray Data	30
Composition and Cell Content	33
Optical Properties	35
THEORETICAL CONSIDERATIONS	36
CONCLUSIONS	41
REFERENCES	42

TABLES

Table		Page
1	Mode and Classification of the Flow Rocks	13
2	Specific Gravities of Several Pleonaste Crystals	22
3	X-ray Powder Pattern	31
4	Chemical Analysis of Pleonaste	33

PLATES

Plate		Following Page
1	Index Map of New Mexico	6
2	Geologic Map of Thesis Area	7
3	Photographs of Basalt Samples	14
4	Photographs of Basalt Samples	15
5	Photographs of Basalt Samples	16
6	Photographs of Basalt Samples	17
7	Photomicrographs of Thin Sections	18
8	Photomicrographs of Thin Sections	19
9	Photomicrographs of Thin Sections	20
10	Drawings of Ideal Crystals	23
11	Drawings of Ideal Crystals	24
12	Photographs of Pleonaste Crystals	25
13	Photographs of Pleonaste Crystals	26
14	Photographs of Pleonaste Crystals	27
15	Photographs of Pleonaste Crystals	28
16	X-ray Powder Photographs	32
17	Phase Diagram	38

INTRODUCTION

Location and Accessibility

The area included in this report comprises about 5 square miles, including parts of Sections 1, 2, 11, 12, 13, 14, 23, and 24, T. 14 S., R. 4 W.; and parts of Sections 6, 7, 18, and 19, T. 14 S., R. 3 W. This area is about 2½ miles southeast of U. S. Highway 85 at the town of Truth or Consequences (Hot Springs), Sierra County, New Mexico, and about 2 miles south of State Highway 52 at the Elephant Butte Dam. A road which leads to Mescal Canyon turns off State Highway 52 at the bridge across the Rio Grande. By following the bed of Mescal Canyon and Salt Canyon (Pl. 2), a point within a mile of the flows can be reached. Mescal Canyon can be followed further to within half a mile of the eastern edge of the flows (Pls. 1, 2).

Physiography

The thesis area lies along the eastern base of North Ridge which forms the northern part of the Caballo Mountains. This ridge rises abruptly, about 1,500 feet, above the considerably dissected lowland on which the area is located. The lowland lies near the head of Mescal Canyon and is dissected into ridges and valleys with a relief of as much as 300 feet. The drainage is east and north into Mescal Canyon (Pl. 2) which joins the Rio Grande just below the Elephant Butte Dam.

Discovery and Utilization

In 1928, two prospectors found some very hard black crystals weathering out of basaltic igneous rocks at the north end of the Caballo Mountains. These crystals caused considerable excitement among the people who saw them; they were certain that the crystals were "black diamonds." Subsequent investigation proved they were not diamonds but a spinel which, with sufficient supply, might replace diamonds in some commercial uses. The financial returns would be small from such a venture and therefore the prospectors abandoned the project. The spinel crystals are scattered through a tough, fine-grained basaltic rock. Mining operations would be difficult, and the number of usable crystals would be small. The good specimens which were recovered were found on the surface of the ground on and near the flows. Even by extensive placer operations no great number of usable crystals could be recovered. At the present time, synthetic spinels with varying physical properties can be manufactured very cheaply. This, of course, makes any attempt at recovery of the natural crystals unfeasible today.

In 1946 the crystals came to the writer's attention, and were collected and identified as pleonaste. The crystals occur in a series of basic lava flows, and several probable dikes. Large crystals of spinel in a flow seemed to be incongruous so a study of the mineral and the flows was undertaken in 1951.

Methods of Study

The mineral was identified by chemical analysis and optical and X-ray properties as pleonaste. The lava flows were studied in thin section with a petrographic microscope.

Subsequent to the beginning of this study similar occurrences of pleonaste were observed in several other localities, two of them a few miles to the north and northeast of the thesis area, and another in the Cabezon Peak area in north-central New Mexico. These localities are marked by stars on the index map (Pl. 1).

Acknowledgments

The writer wishes to gratefully acknowledge the help of the thesis committee, Dr. Carl W. Beck, Dr. J. Paul Fitzsimmons, and Dr. Vincent C. Kelley; especial thanks are due Dr. Beck, under whose direction this thesis was written. The writer acknowledges the assistance of George Brunton in some of the field and laboratory work.

GENERAL GEOLOGY

The oldest rock in the mapped area is that of the Magdalena group of Pennsylvanian age. The Magdalena group makes up most of North Ridge immediately to the west of the area. The Magdalena group is about 1,200 feet thick, and consists dominantly of limestone with lesser amounts of shale and sandstone. The Magdalena is overlain by the Manzano group of Permian age, consisting of the Abo formation (550 feet thick), the Yeso formation (750 feet thick), and the San Andres formation (760 feet thick). The Abo is a red-brown formation consisting of shale and sandstone of continental origin. The Yeso consists of tannish-brown siltstone and sandstone, gypsum, and some limestone of both marine and continental origin. The San Andres formation is dominantly a gray marine limestone, but with lesser amounts of shale and sandstone. Disconformably overlying the Manzano group is the Dakota sandstone (250 feet thick), Mancos shale (400 feet thick), and the Mesaverde formation 2,500 feet thick), all of late Cretaceous age. The Dakota sandstone is composed of tan and buff sandstone with a small amount of shale. The Mancos is a greenish shale. The Mesaverde formation consists mostly of alternating sandstone and shale units with local beds of coal.*

The above Paleozoic and Mesozoic formations are generally tilted eastwardly in the mapped area at steep to

---

*Kelley, V. C., oral communication.

moderate angles. In late Pliocene or early Pleistocene time the upturned edges of the older rocks were widely beveled by a pediment which encroached upon the range from the Jornada del Muerto Valley. The basaltic flows containing the pleonaste lie upon this erosion surface near its junction with the mountains (Pl. 2).

The northernmost flows all dip very gently to the east, and the contact between them and the underlying moderately dipping strata is remarkably level and uniform. The several large bodies of lava in this section are fairly uniform in thickness and attitude. They are composed of four separate flows, with a total thickness of about twenty feet--the first flow is three feet thick; the second, six feet; the third, seven feet; and the fourth, about four feet. The top flow is eroded from most of the area, and much of the third flow is gone. The two bottom flows seem to be present in all of the northern outcrops.

In the southern section of the mapped area, in the smaller patches of lava, the contact with the underlying sediments is very irregular and the flows themselves range greatly in thickness and attitude. A number of gentle folds in the lava were apparently caused by a post-flow folding.

An old pediment covers the northernmost flow and a similar remnant covers part of the sediments in the southern part of the area. The present stream gradient is considerably lower and steeper than these old remnants of dep-

osition which were largely removed and deeply eroded by the rejuvenated streams (Pl. 2).

PLATE 1

Index Map of New Mexico

Stars represent known pleonaste localities outside of thesis area.


Santa Fe
Albuquerque
NEW MEXICO
Truth or
Consequences
Thesis area

PLATE 2

GEOLOGIC MAP OF THESIS AREA

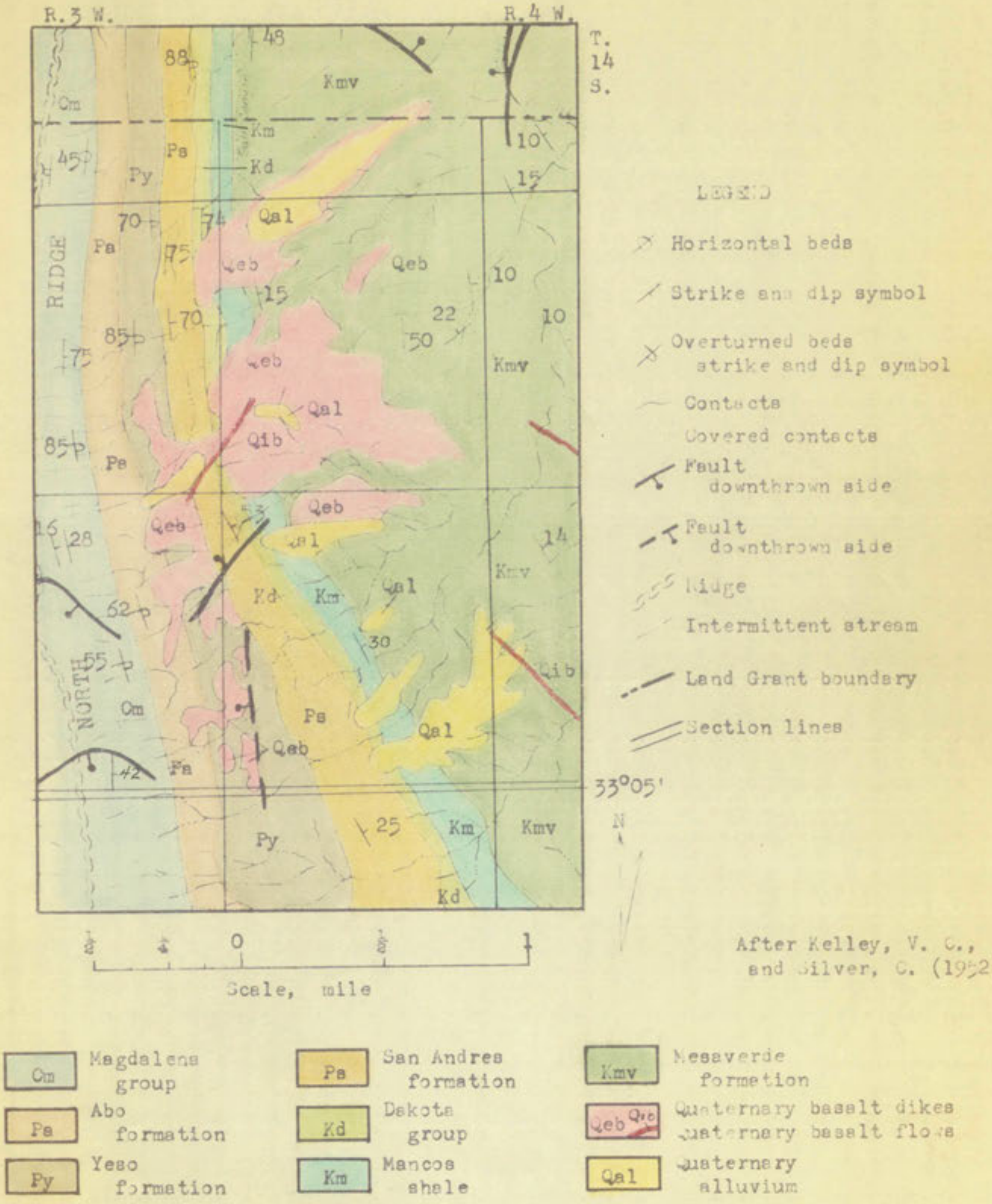

After Kelley, V. C., and Silver, C. (1952)

PETROGRAPHY OF THE FLOW ROCKS

Samples of the flow rocks were taken at chosen intervals throughout the thesis area. No attempt was made to delineate and correlate the various flow layers in one part of the area with the flow layers in other parts. A great number of samples were taken; studied under magnifications of 6 to 40 diameters; and divided into five groups on the basis of the appearance of the weathered surface, fresh surface, texture, and those minerals large enough to be seen. Thin sections were made from representative samples of each of the five types, and studied with a petrographic microscope. The modes, or percentages of the mineral components, were calculated by use of a Wentworth stage on the microscope. The linear traverses on a Wentworth stage are proportional to the surface areas, which in turn are proportional to the volumes of the constituent minerals. Following are macroscopic and microscopic descriptions of each sample:

Sample 1 (Pl. 3, Fig. 1).

This rock is dense, dark gray, porphyritic, with phenocrysts composed of yellowish olivine, a black amphibole, and spinel. The groundmass ranges from very fine grained to aphanitic. The phenocrysts range in size from less than 1 mm to as large as 20 mm. in diameter. The surface weathers to a gray-buff color with an earthy appearance.

Thin-section studies showed a groundmass of glass and unidentifiable crystallites around randomly oriented, twinned plagioclase laths, giving the rock a felty or hyalo-ophitic texture. Many small grains of augite and hornblende occur in the groundmass, and some of the larger grains show a core of olivine. Many small grains of an opaque mineral, probably magnetite, are usually associated with the olivine, augite and hornblende grains. Large euhedral and subhedral olivine phenocrysts have a corona of serpentine, and most of the cracks contain serpentine (Pl. 7, Fig. 1). Small grains, usually single crystals, of anhedral nepheline occur near the rims of the olivine phenocrysts, and occasionally scattered through the groundmass. The occasional phenocrysts of augite are dark greenish-brown with a darker brown pleochroic halo of hornblende. The spinel occurs as large euhedral and subhedral grains with sharp boundaries, dark emerald green in the center and lighter green around the edges. They exhibit two prominent directions of parting at angles of 90 degrees (Pl. 7, Fig. 2). The mode of this rock is given in table 1.

In Johannsen's classification, sample would be 3316E, which is unnamed. The hypabyssal equivalent (3316H) is madeirite (Johannsen, Vol. IV, pp. 69, 73-74).

Sample 2 (Pl. 3, Fig. 2; Pl. 4, Figs. 1a, 2).

This rock is fine grained, porphyritic, vesicular, dark gray-brown, with phenocrysts of black pyroxene, spinel

and yellow-brown olivine. The phenocrysts range in size from less than 1 mm to 20 mm in diameter. The vesicles are small, irregular, and elongate in one direction. This rock weathers to a buff-colored, earthy, porous mass.

Thin section studies showed a groundmass of crystallites and microlites of plagioclase around randomly oriented, twinned plagioclase laths, similar to sample 1. Many small grains of augite and hornblende occur in the groundmass, some with cores of olivine. Nepheline is common, and there are minor amounts of riebeckite, clinoenstatite, aegirine, analcime and biotite. The nepheline is found in large aggregates, usually adjoining the olivine phenocrysts, and is composed of small anhedral grains with a random orientation. A small percentage is in single grains in the groundmass (Pl. 9, Figs. 1, 2). The minor accessories are in small grains scattered through the groundmass. The mode of this rock is given in table 1.

In Johannsen's classification, sample 2 would be the effusive equivalent of kylite (3320P) (Johannsen, Vol. IV, p. 226), which would be similar to Lehman's atlantite (3320E) (Johannsen, Vol. IV, p. 240).

Sample 3 (Pl. 4, Figs. 1b, 1c; Pl. 5, Figs. 1, 2).

This rock is medium to dark brown, porphyritic, vesicular, fine grained to aphanitic, with small phenocrysts of olivine and spinel and an occasional phenocryst of pyroxene. There are a few large, euhedral crystals of spinel in and yellow-brown olivine. The phenocrysts range in size from less than 1 mm to 20 mm in diameter. The vesicles are small, irregular, and elongate in one direction. This rock weathers to a buff-colored, earthy, porous mass.

Thin section studies showed a groundmass of crystallites and microlites of plagioclase around randomly oriented, twinned plagioclase laths, similar to sample 1. Many small grains of augite and hornblende occur in the groundmass, some with cores of olivine. Nepheline is common, and there are minor amounts of riebeckite, clinoenstatite, aegirine, analcime and biotite. The nepheline is found in large aggregates, usually adjoining the olivine phenocrysts, and is composed of small anhedral grains with a random orientation. A small [illegible] is in size as grains in the groundmass (Pl. 9, Figs. 1, 2). The minor accessories are in small grains scattered through the groundmass. The mode of this rock is given in table 1.

In Johannsen's classification, sample 2 would be the effusive equivalent of ijolite (3520E) (Johannsen, Vol. IV, p. 225), which would be similar to [illegible] (3320E) (Johannsen, Vol. IV, p. [illegible]).

Sample 3 (Pl. 4, Figs. 1b, 2a; Pl. 5, Figs. 1, 2).

This rock is medium to dark brown, porphyritic, vesicular, fine grained to aphanitic, with small phenocrysts of olivine and spinel and an occasional phenocryst of pyroxene. There are a few large, euhedral crystals of spinel in this rock (Pl. 13, Figs. 1, 3b; Pl. 14, Figs. 1b, 1c; Pl. 15, Figs. 1, 2).

Thin sections of this rock show textures and minerals similar to those of sample 1. The augite and hornblende are more prominent and more widely scattered through the groundmass; the phenocrysts are, in general, smaller and the olivine shows a greater amount of alteration to serpentine and hornblende on the larger phenocrysts, and to hornblende and augite on the smaller grains. There is a greater percentage of larger grains of opaque minerals. There is also a higher percentage of glass. The mode of this rock is given in table 1.

Johannsen's classification of this rock would be 3316E, the same as sample 1.

Samples 4 and 5 are of this same rock at different orientations. The descriptions and modes are the same.

Sample 6 (Pl. 4, Fig. 1d; Pl. 6, Fig. 1).

This sample is a gray and light brown rock which weathers to a mottled rich brown and light gray; otherwise it is the same as sample 3.

The thin sections are identical with those of samples 3, 4, and 5.

Sample 7 (Pl. 6, Fig. 2).

This sample is a dark brown, vesicular, aphanitic to fine grained rock which grades into scoria in places. The scoria weathers to a medium brown, and the vesicular this rock (Pl. 13, Figs. 1, 3a; Pl. 14, Figs. 1b, 1c; Pl. 15, Figs. 1, 2).

Thin sections of this rock show textures and minerals similar to those of sample 1. The augite and hornblende are more prominent and more widely scattered through the groundmass; the phenocrysts are, in general, smaller and the olivine shows a greater amount of alteration to serpentine and hornblende on the larger phenocrysts, and to hornblende and augite on the smaller grains. There is a greater percentage of larger grains of opaque minerals. There is also a higher percentage of glass. The mode of this rock is given in Table 1.

Johannsen's classification of this rock would be 3316E, the same as sample 1.

Samples 4 and 5 are of this same rock at different orientations. The descriptions and modes are the same.

Sample 6 (Pl. 4, Fig. 1d; Pl. 6, Fig. 1).

This sample is a grey and light brown rock which weathers to a mottled rich brown and light grey; otherwise it is the same as sample 3.

The thin sections are identical with those of samples 3, 4, and 5.

Sample 7 (Pl. 6, Fig. 2).

This sample is a dark brown, vesicular, aphanitic to fine grained rock which grades into scoria in places. The scoria weathers to a medium brown, and the vesicular-rock weathers to a medium and light earthy brown.

Thin sections show a groundmass composed largely of very small laths and microlites of labradorite, crystallites of plagioclase (?), and glass. Augite and hornblende occur as dark brown, shadow-like masses, altering to serpentine. Olivine occurs in the largest grains, most of which are altered to serpentine and hornblende-augite, with only small residual cores of olivine. A few very small irregular grains of brownish-green spinel, and many small opaque grains are scattered through the groundmass. The mode and classification of this rock is given in table 1.

TABLE 1

Mode and Classification of the Flow Rocks

Minerals	Samples			
	1	2	3	7
Labradorite	30.8	23.3	19.7	24.3
Nepheline	1.2	7.3	3.3	2.1
Augite	12.4	5.7	18.2	19.3
Hornblende	6.2	4.3	7.0	10.8
Olivine	32.0	30.8	21.4	15.3
Opacites	1.0	2.1	2.6	10.8
Spinel	1.0	1.1	1.3	0.3
Serpentine	7.1	6.4	13.0	9.0
Accessories	6.4	16.0	10.5	3.0
Glass	1.8	2.0	3.0	4.0
Total	99.9	99.0	100.0	98.9
Classification	3316	3320	3316	3316

PLATE 3

Photographs of Basalt Samples

Figure 1. Photograph of specimen of
basalt, sample 1. :X1.
S = spinel crystal.

Figure 2. Photograph of specimen of
basalt, sample 2. :X$\frac{1}{2}$.
S = spinel crystal.

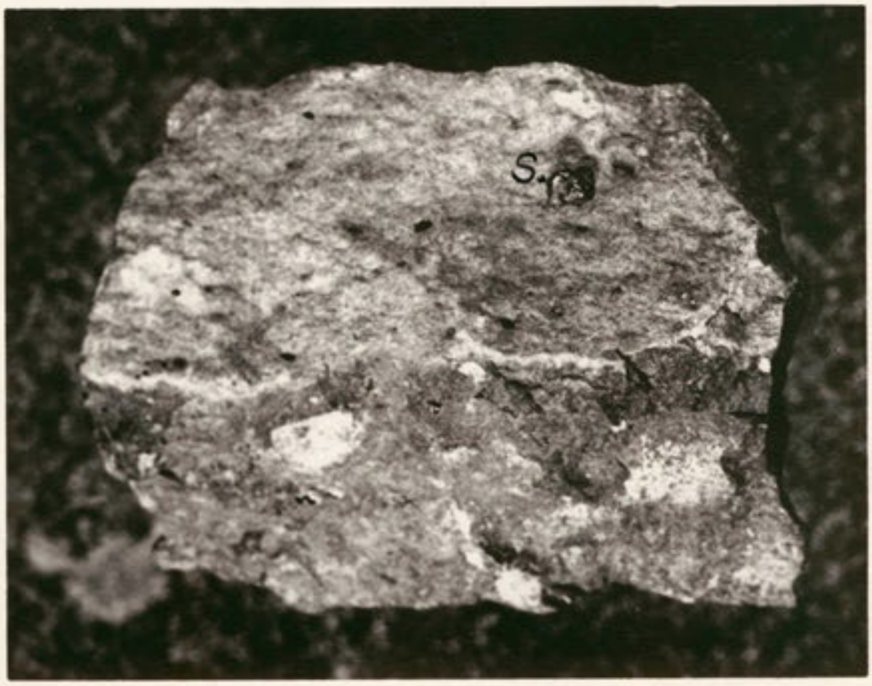

Figure 1

Figure 2

PLATE 4

Photographs of Basalt Samples

Figure 1. Photograph of specimens of basalt. a = sample 2, b and c = sample 3, d = sample 6. :X¼.

Figure 2. Photograph of specimen of basalt, sample 2. :X1.
S = spinel crystal.
P = pyroxene phenocryst.

Figure 1

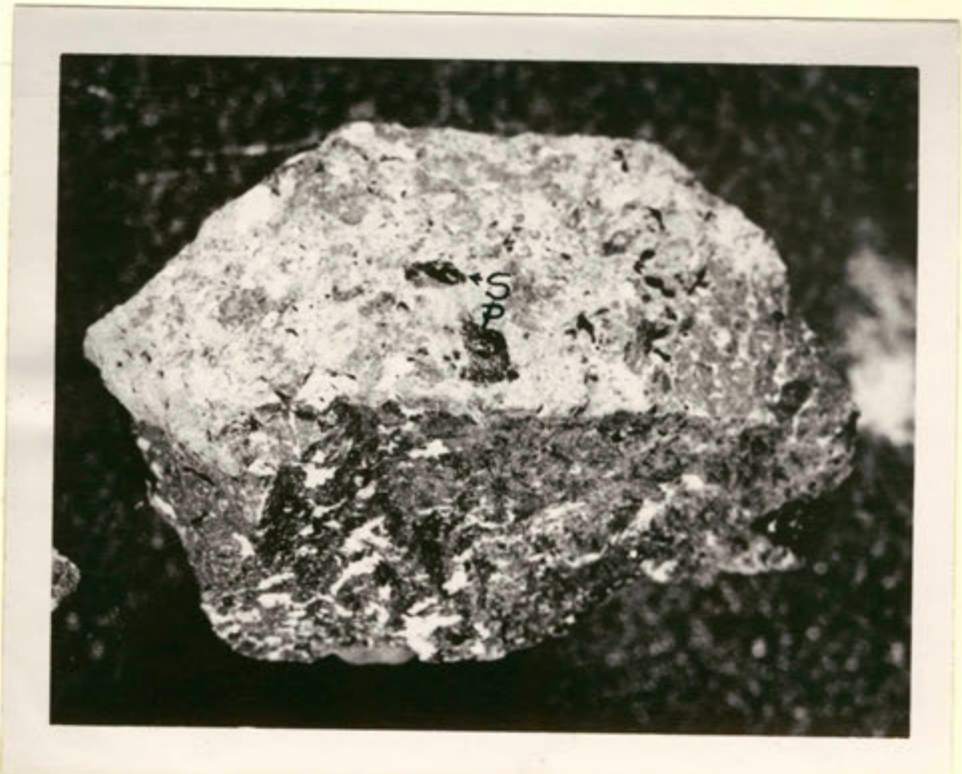

Figure 2

PLATE 5

Photographs of Basalt Samples

Figure 1. Photograph of specimen of basalt, sample 3. :X1. S = spinel crystal.

Figure 2. Photograph of specimen of basalt, sample 3. :X1.

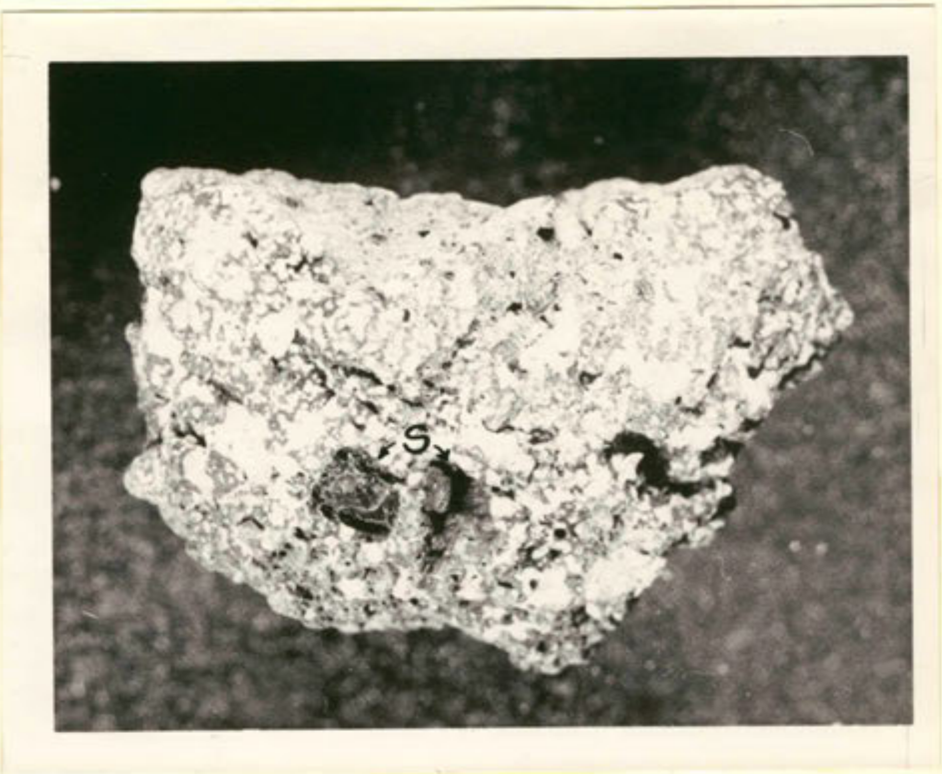

Figure 1

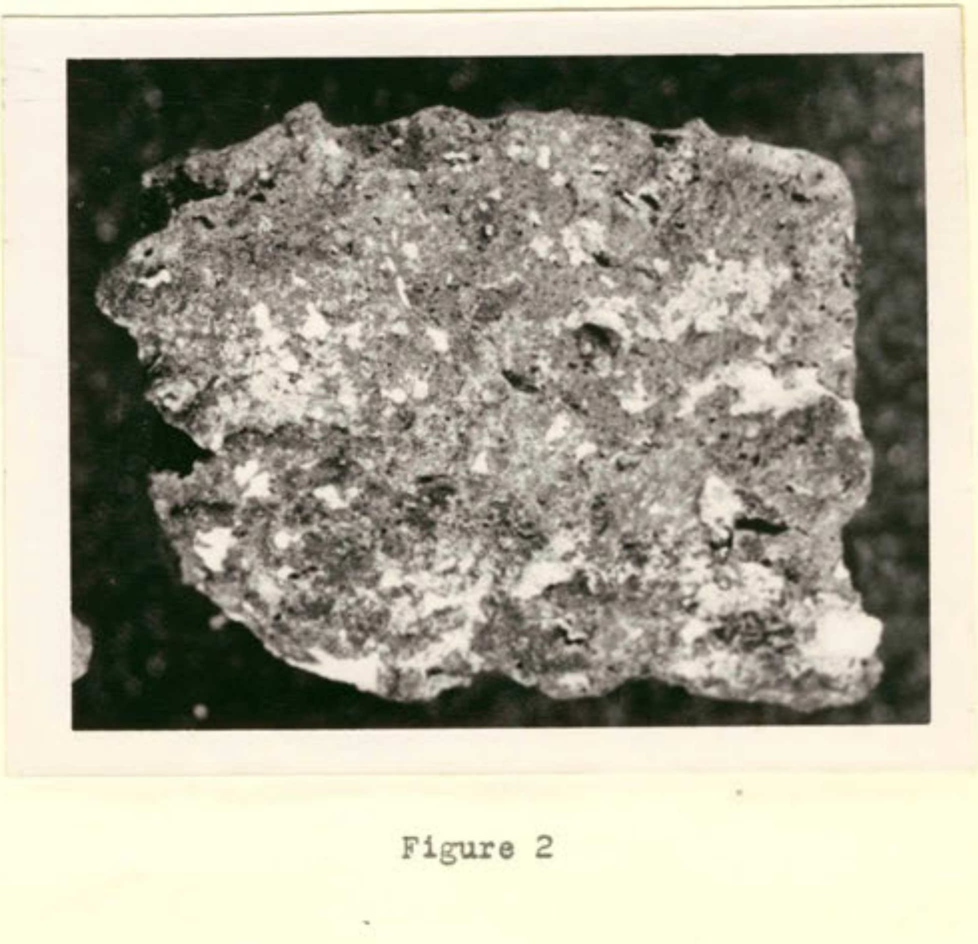

Figure 2

PLATE 6

Photographs of Basalt Samples

Figure 1. Photograph of specimen of basalt, sample 6. :X1. S = spinel crystal.

Figure 2. Photograph of specimen of basalt, sample 7. :X1.

Figure 1

Figure 2

PLATE 7

Photomicrographs of Thin Sections

Figure 1. Photomicrograph of thin section from sample 1. Plane light. :X100.
O = olivine crystal showing serpentinization.

Figure 2. Photomicrograph of thin section from sample 2. Plane light. :X35.
Spinel crystal showing two colors and cubic parting.

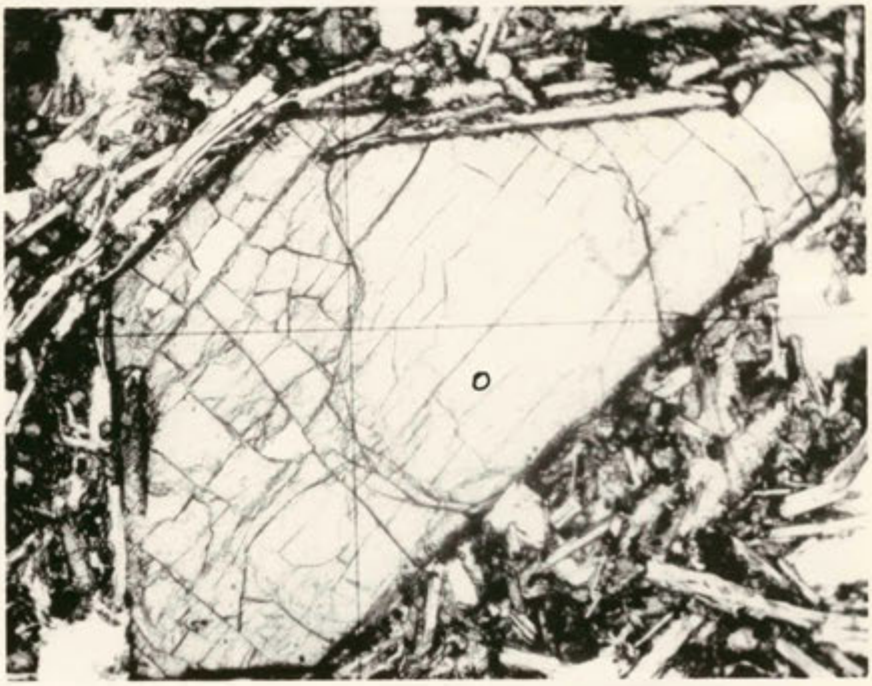

Figure 1

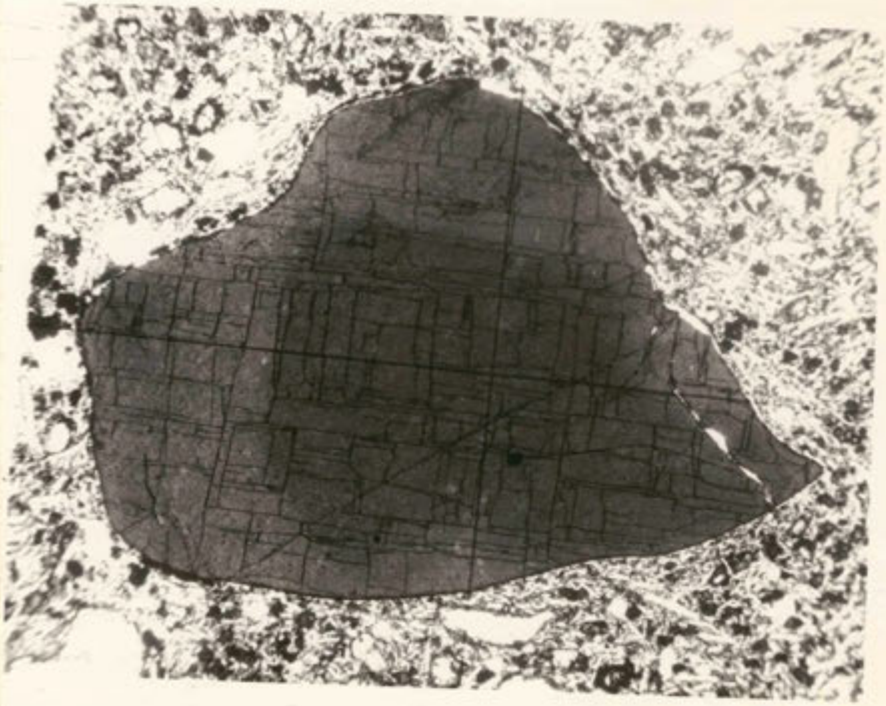

Figure 2

PLATE 8

Photomicrographs of Thin Sections

Figure 1. Photomicrograph of thin section of basalt sample showing typical arrangement of minerals. Plane light. :X200.
O = olivine.
P = plagioclase lath.

Figure 2. Same as figure 1, crossed nicols.

Figure 1

Figure 2

PLATE 9

Photomicrographs of Thin Sections

Figure 1. Photomicrograph of thin section from sample 2. Plane light. X100.
S = spinel.
O = olivine.
N = nepheline.
Se = serpentine.

Figure 2. Same as figure 1, crossed nicols.

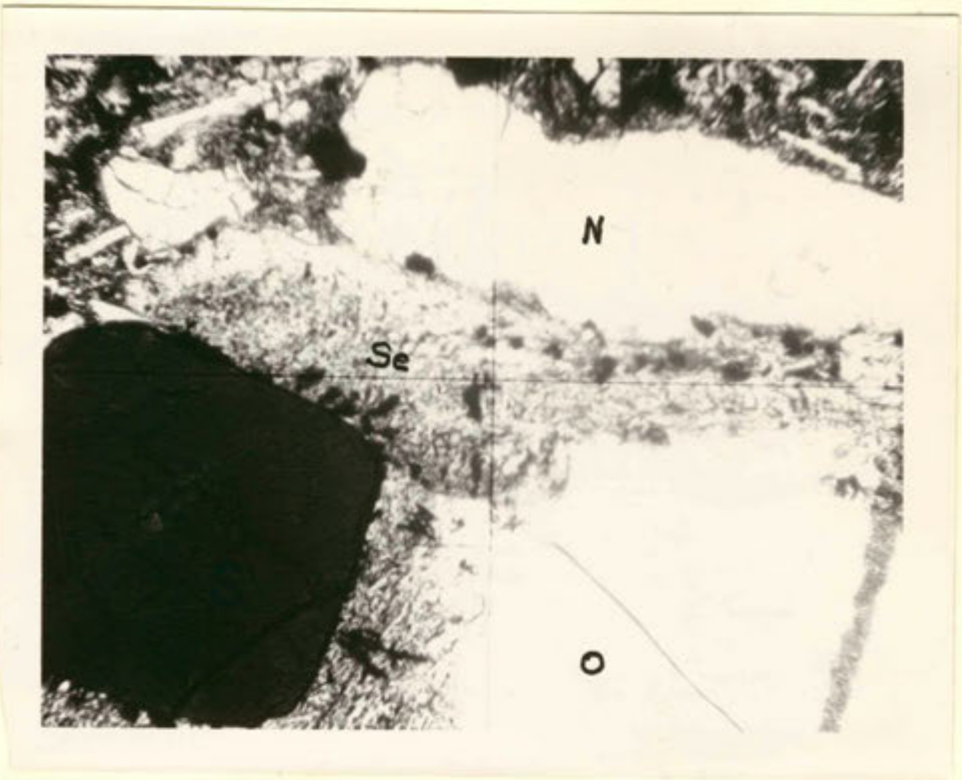

Figure 1

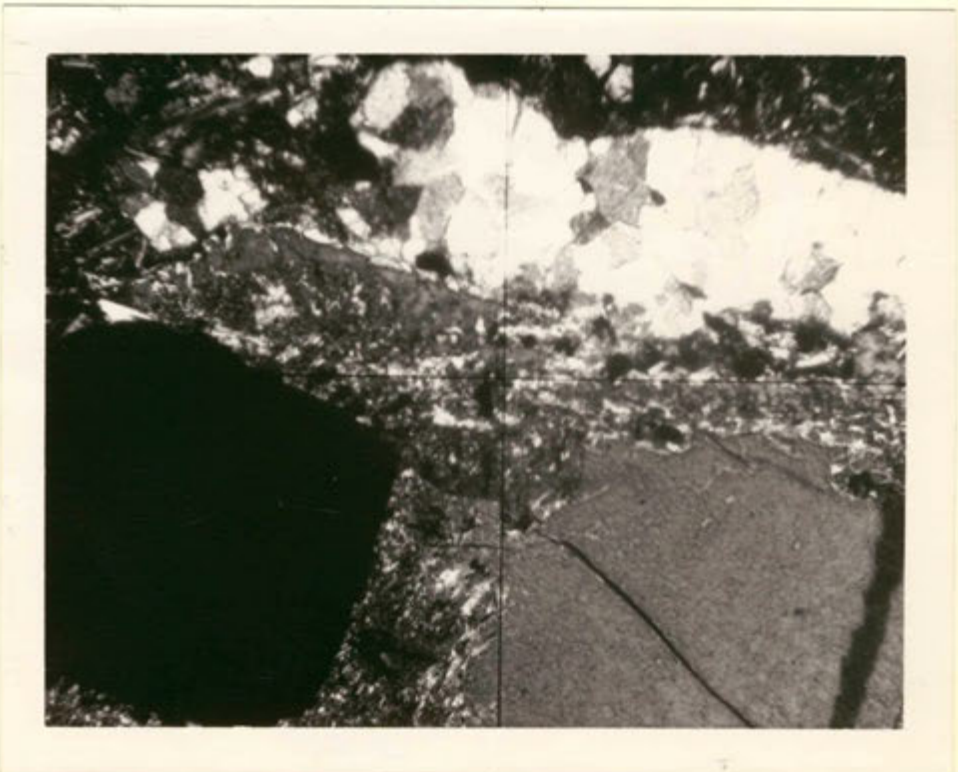

Figure 2

MINERALOGY OF PLEONASTE

Crystallography

Isometric, hexoctahedral. It is found usually in octahedrons, sometimes with dodecahedral truncations, rarely with cubic truncations (Pls. 10, 11, 12, 13, 14). Most specimens are malformed, with rounded edges (Pl. 12, Fig. 2); some have pitted surfaces (Pl. 13, Fig. 1); most of them are incomplete crystals. Twins are rare, but when found are spinel twins; that is, the twin axis is the axis of three-fold symmetry.

Physical Properties

The color is dark green and brown; diaphaneity, nearly opaque; fracture, conchoidal; tenacity, brittle; luster, dull on external surface, vitreous to splendent on fractures; streak, white; hardness, 8.

The specific gravity of the mineral was determined with a Jolly balance, which measures the relative weight of the mineral in air and in water. The equation used is:

$$\text{Specific Gravity} = \frac{\text{Weight in Air}}{\text{Weight in Air} - \text{Weight in Water}}$$

The specific gravity for this pleonaste ranges from 3.8280 to 3.8839 and averages 3.8563 (Table 2).

The theoretical specific gravity of a crystal may be calculated from the equation:

$$\text{Density} = \frac{\text{Weight}}{\text{Volume}}$$

TABLE 2

Specific Gravities of Several Pleonaste Crystals

Crystal No.	Measurements			
	1st	2nd	3rd	Average
1	3.8491	3.8508	3.8390	3.8463
2	3.8849	3.8757	3.8647	3.8751
3	3.8250	3.8190	3.8400	3.8280
4	3.8566	3.8579	---	3.8572
5	3.8774	3.8905	---	3.8839
6	3.8384	3.8308	---	3.8346
7	3.8417	---	---	3.8417
8	3.8737	---	---	3.8737
9	3.8656	---	---	3.8656

Average = 3.8563

PLATE 10

Drawings of Ideal Crystals

Figure 1. Drawing of an ideal octahedron.
Clinographic projection.

Figure 2. Drawing of an ideal octahedron
with dodecahedral truncations.
Clinographic projection.

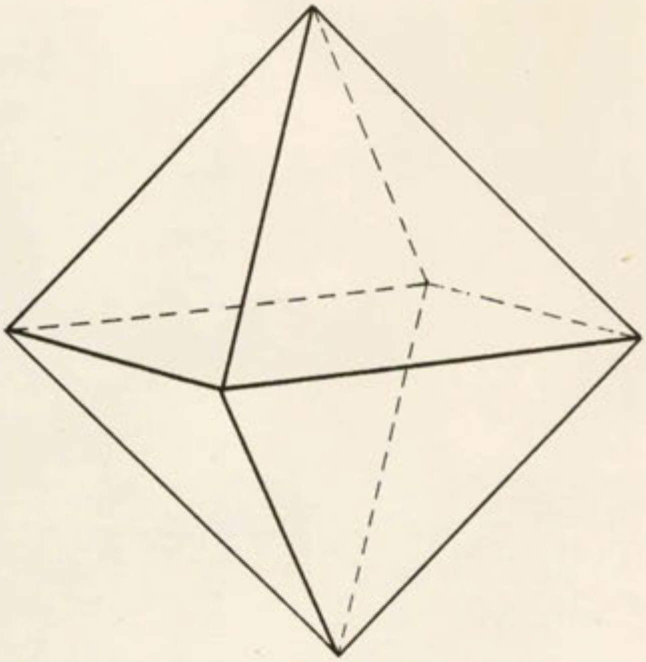

Figure 1.

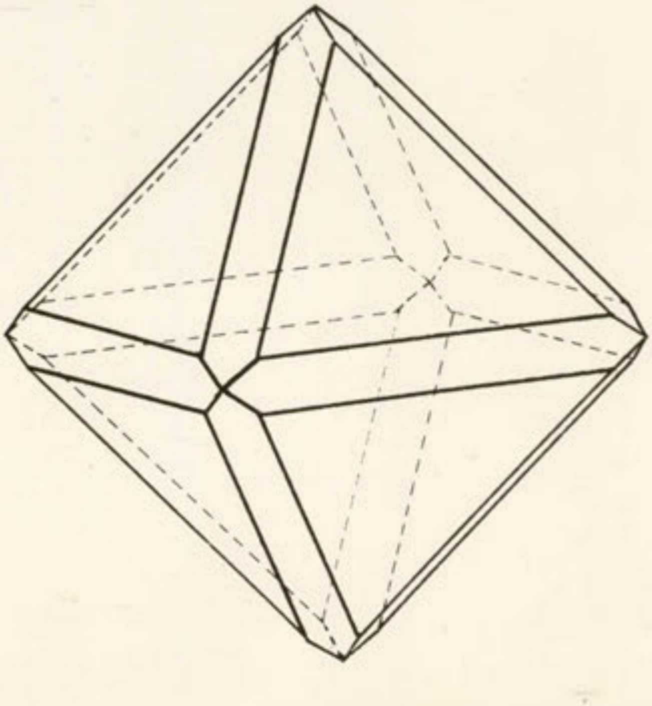

Figure 2.

PLATE 11

Drawings of Ideal Crystals

Figure 1. Drawing of an ideal octahedron with dodecahedral truncations. Clinographic projection.

Figure 2. Portrait of an actual spinel crystal in an ideal drawing.

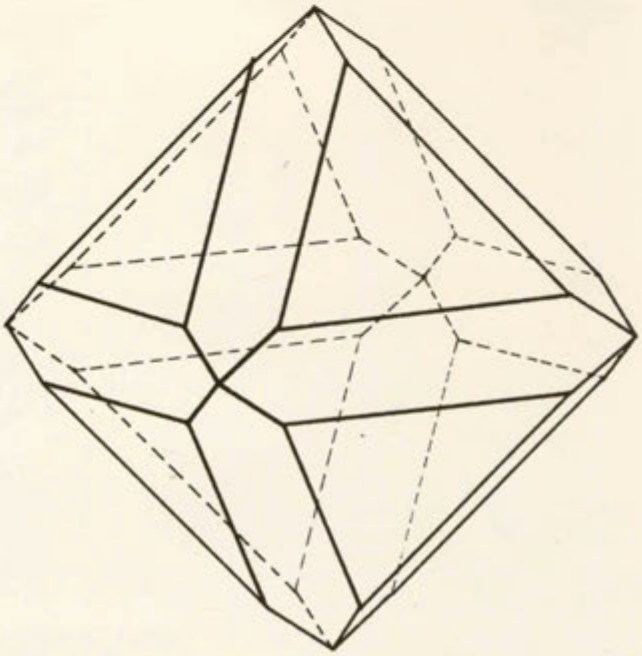

Figure 1.

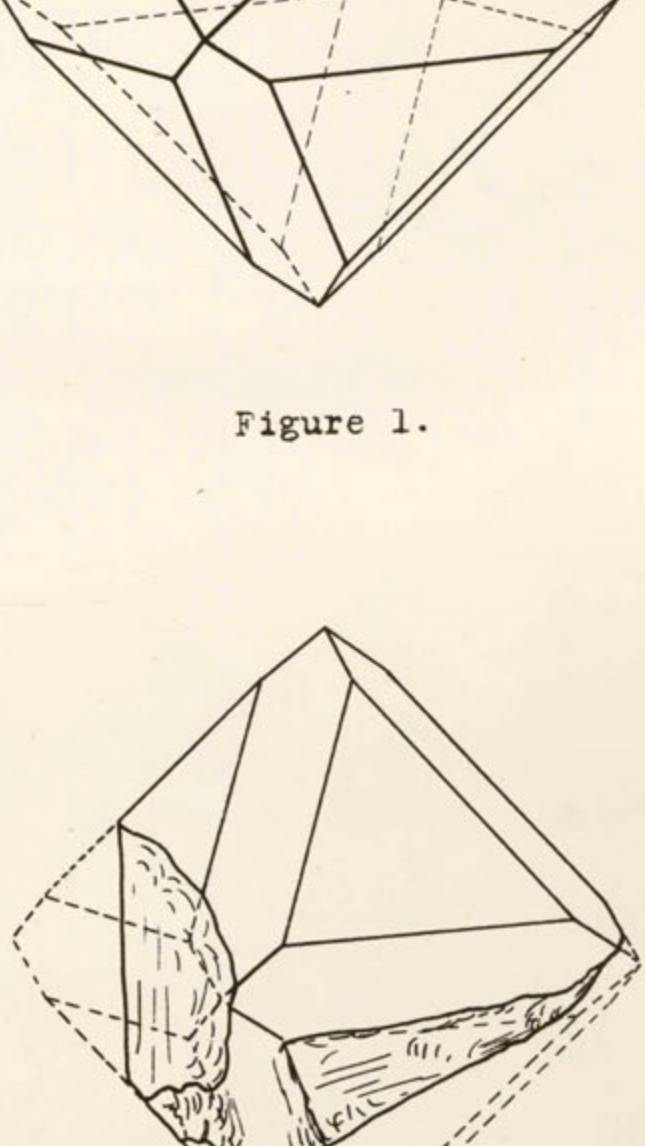

Figure 2.

PLATE 12

Photographs of Pleonaste Crystals

Figure 1. Photograph of pleonaste crystals from basalt. Scale in inches on photograph.

Figure 2. Photograph of pleonaste crystals from basalt. :X4

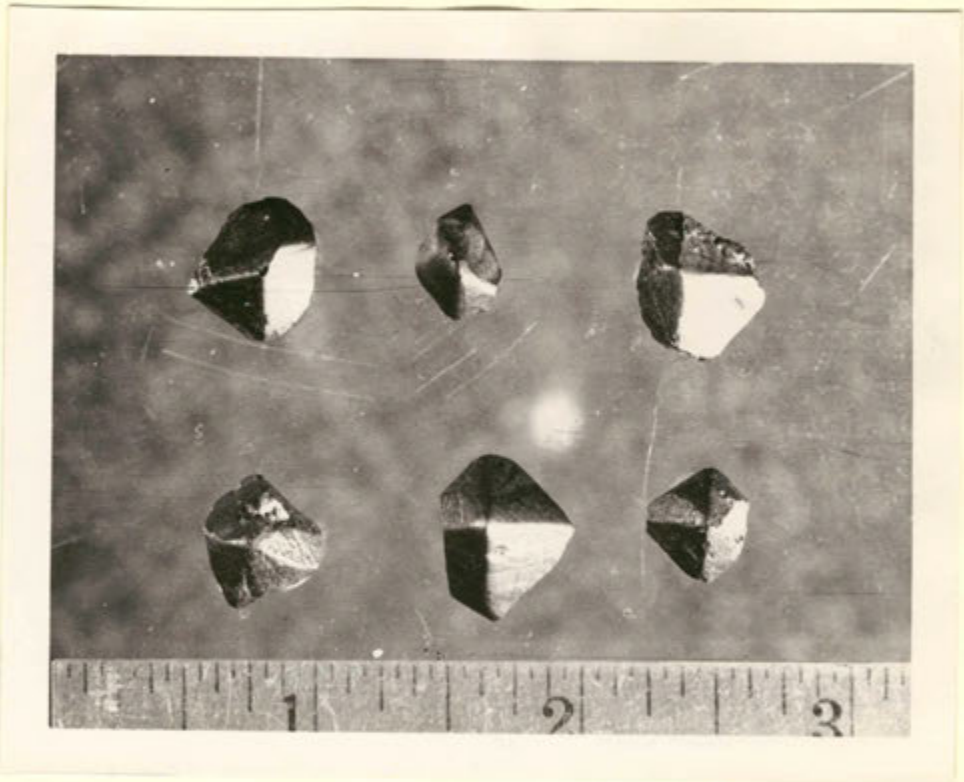

Figure 1

Figure 2

PLATE 13

Photographs of Pleonaste Crystals

Figure 1. Photograph of pleonaste crystal showing pitted surface. :X2.

Figure 2. Photograph of pleonaste crystal from basalt. :X3.

Figure 3. Photograph of four pleonaste crystals (a, b, c, and d) from basalt. :X2.

PLATE 13

Photographs of Pleonaste Crystals

Figure 1. Photograph of pleonaste crystal showing pitted surface. :X2.

Figure 2. Photograph of pleonaste crystal from basalt. :X3.

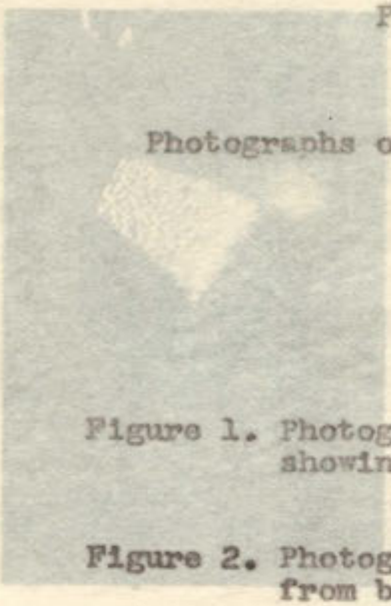

Figure 1

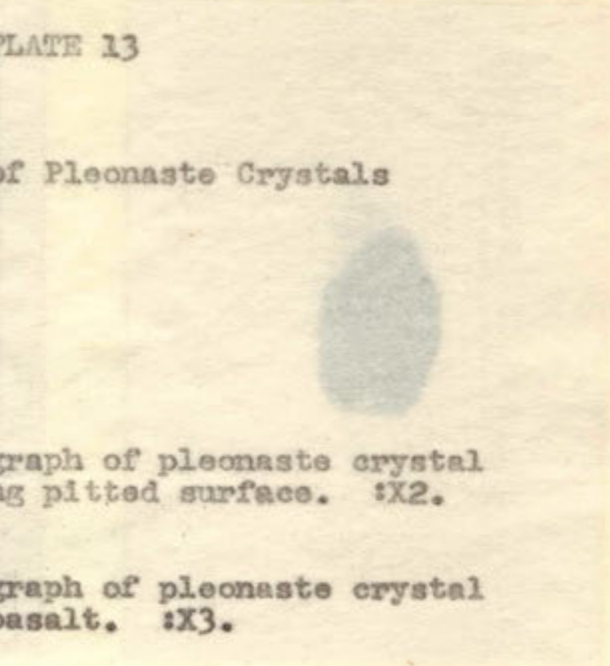

Figure 2

Figure 3. Photograph of four pleonaste crystals (a, b, c, and d) from basalt. :X2.

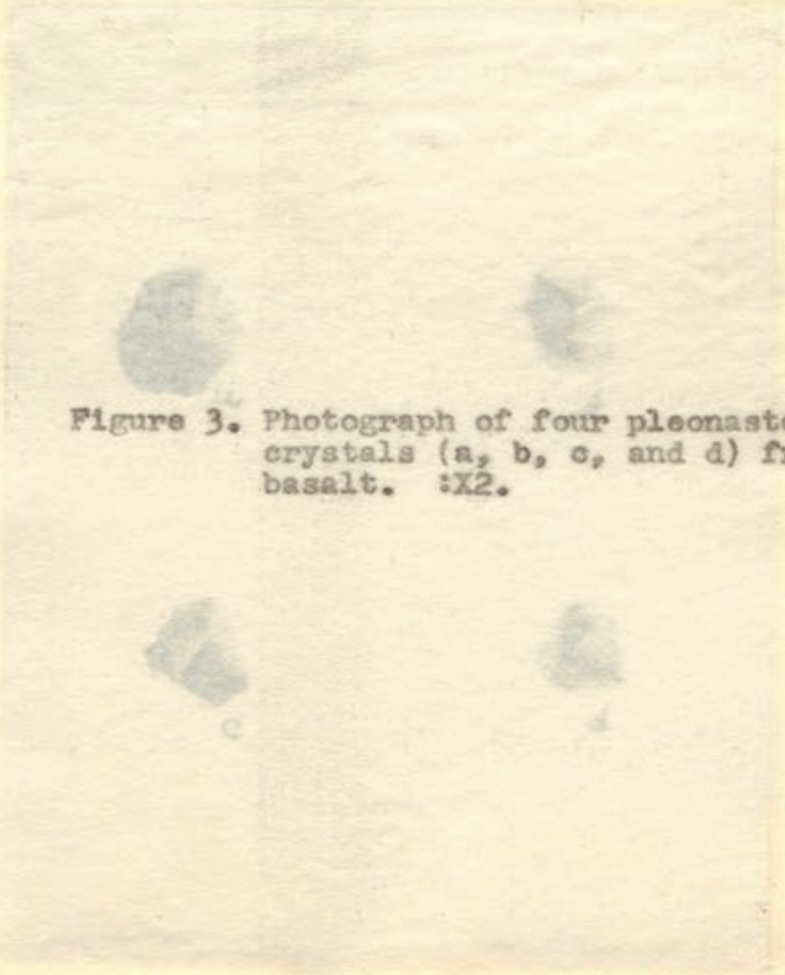

Figure 3

Figure 1

Figure 2

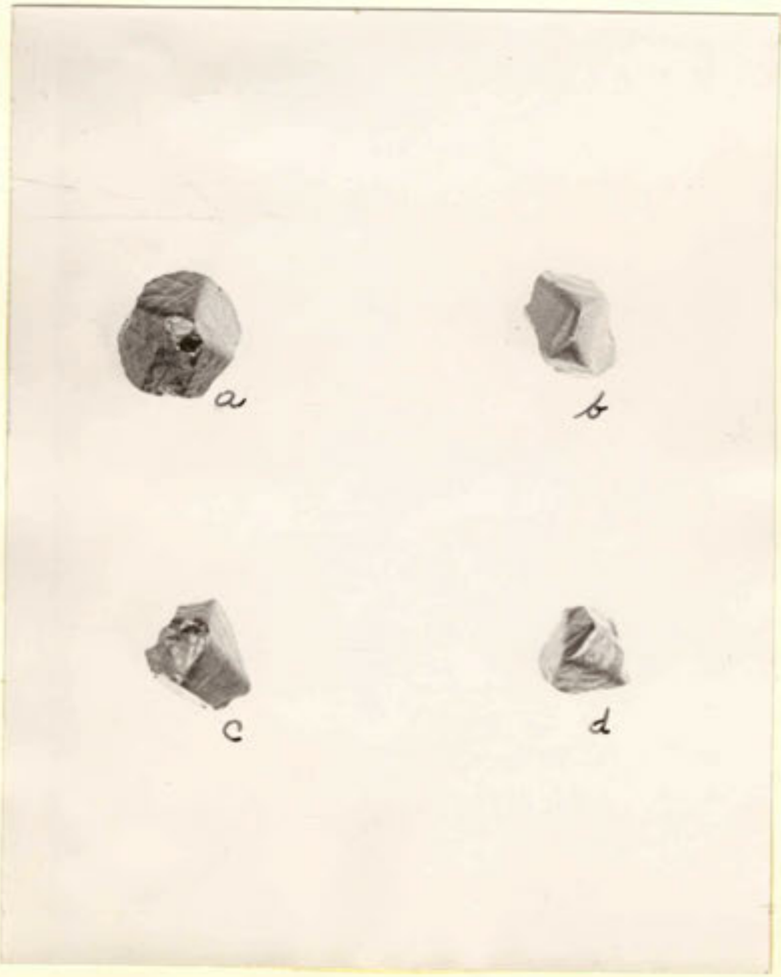

Figure 3

PLATE 14

Photographs of Pleonaste Crystals

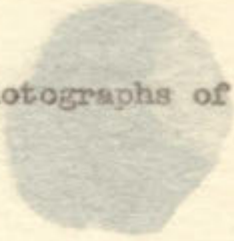

Figure 1

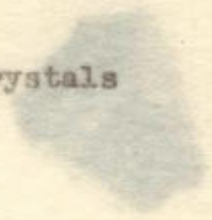

Figure 2

Figure 1. Photograph, enlargement of fig. 3a, Pl. 13. :X4.

Figure 2. Photograph, enlargement of fig. 3c, Pl. 13. :X4.

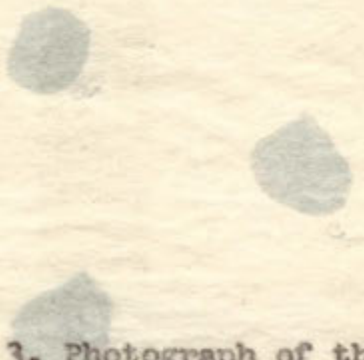

Figure 3

Figure 3. Photograph of three pleonaste crystals from basalt (a, b, and c). :X1.

Figure 4. Photograph, enlargement of fig. 3a above. :X4.

Figure 4

Figure 1

Figure 2

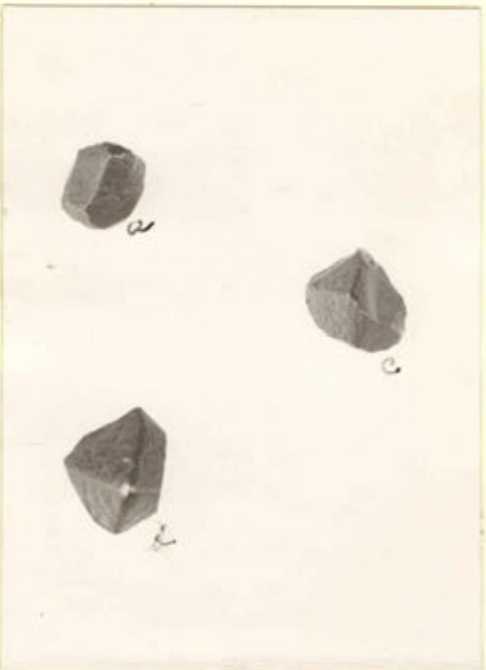

Figure 3

Figure 4

PLATE 15

Photographs of Pleonaste Crystals

Figure 1. Photograph, enlargement of fig.
3b, Pl. 14. :X4.

Figure 2. Photograph, enlargement of fig.
3c, Pl. 14. :X4.

Figure 1

Figure 2

The weight is the product of the molecular weight of the chemical unit of which the crystal is composed times the number of such units per unit crystal, times the factor 1.649×10^{-24} which changes units of atomic weight into grams. The volume is the volume of the unit crystal. In the isometric system the density of the crystal is:

$$\rho = n\frac{M \times 1.649 \times 10^{-24}}{a_0^3} \qquad \text{(Davey, p. 35)}$$

where M is the molecular weight, a_o is the edge of the unit cube in centimeters, and n is the number of points associated with the unit cube in the crystal lattice. n is 1 for a simple cube, 2 for a body-centered cube, 4 for a face-centered cube, and 8 for a diamond cube.

a_o was determined from X-ray powder photographs of the mineral by the equation:

$$n\lambda = 2d \sin \theta \qquad \text{(Buerger, p. 98)}$$

where n is the order of the reflection, λ is the wave length of the X-ray beam, d is the atomic spacing (a_o), and θ is the angle the reflected X-ray beam makes with the plane of the crystal.

M was determined in the following way:

M = percentage molecular weights of $FeO + MgO + Fe_2O_3 + Al_2O_3$

$$FeO = 71.85 \times \frac{16.07}{33.23} = 34.74$$

$$MgO = 40.32 \times \frac{17.16}{33.23} = 20.82$$

The weight is the product of the molecular weight of the chemical unit of which the crystal is composed times the number of such units per unit crystal, times the factor 1.649×10^{-24} which changes units of atomic weight into grams. The volume is the volume of the unit crystal. In the isometric system the density of the crystal is:

$$\rho = n \frac{M \times 1.649 \times 10^{-24}}{a_0^3} \qquad \text{(Davey, p. 35)}$$

where M is the molecular weight, a_0 is the edge of the unit cube in centimeters, and n is the number of points associated with the unit cube in the crystal lattice; n is 1 for a simple cube, 2 for a body-centered cube, 4 for a face-centered cube, and 8 for a diamond cube.

a_0 was determined from X-ray powder photographs of the mineral by the equation:

$$n\lambda = 2d \sin\theta \qquad \text{(Wherry, 1936)}$$

where n is the order of the reflection, λ is the wave length of the X-ray beam, d is the atomic spacing (A.), and θ is the angle the reflected X-ray beam makes with the plane of the crystal.

M was determined in the following way:

M = percentage molecular weights of FeO + MgO + ZnO + Al_2O_3

$$FeO = 71.85 \times \frac{18.07}{33.23} = 39.07$$

$$MgO = 40.32 \times \frac{17.16}{33.23} = 20.82$$

$$Fe_2O_3 = 159.7 \frac{1.60}{66.67} = 3.83$$

$$Al_2O_3 = 101.94 \frac{65.07}{66.67} = 99.49$$

$$M = 158.88$$

Substituting figures in the equation on page 29, we get:

$$\rho = 8 \frac{158.88 \times 1.649 \times 10^{-24}}{(8.12)^3 \times 10^{-24}} = 8 \frac{262.0}{535.4} = 3.9144$$

The calculated specific gravity, 3.9144, compares favorably with the average measured specific gravity, 3.8563.

Structural Crystallography

The mineral spinel is the type mineral for the spinel group, all of which have the same isometric atomic structures. For spinel the structure may be described as having the O atoms arranged on a face-centered cubic lattice with the Mg atoms lying in the center of tetrahedral groups of four atoms, while the Al atoms are each surrounded by a group of six O atoms. Space group, Fd3m; a_o, 8.12 A; unit cell content, 8 (Winchell, Part II, p. 81).

X-ray Data

Because the mineral is isometric, with equal axes at 90 degrees to each other, the only X-ray photographs taken were powder pictures. The pleonaste was mixed with a small amount of halite so a check could be made on the

measurements taken from the X-ray films. Photographs were taken with both CuK_α and FeK_α radiation (Pl. 16). Tabulated results of these photographs are shown in table 3 below.

TABLE 3

X-ray Powder Pattern

Isometric, Fd3m; a_0 = 8.12 A

FeK_α Radiation			CuK_α Radiation		
I	2θ	d	I	2θ	d
1	23.75	4.710	2	18.85	4.700
½	36.15	3.120	4	30.95	2.890
2	39.35	2.877	10	36.55	2.450
½	42.05	2.700	5	44.45	2.030
10	46.45	2.456	1	55.15	1.660
½	47.15	2.420	5	58.85	1.560
4	56.80	2.036	6	64.65	1.440
½	58.95	1.970	1	76.65	1.240
1	71.25	1.663	2	83.85	1.150
3	76.25	1.569	½	90.15	1.080
½	77.15	1.553	1	93.75	1.050
6	84.55	1.440	½	98.95	1.010
½	89.45	1.376	½	101.35	0.996
2	100.70	1.258	1	110.75	0.938
1	111.15	1.170		110.35	0.938
2	114.70	1.149	½	119.75	0.890
	115.05	1.150	1	129.45	0.851
½	116.70	1.137		130.15	0.851
1	126.10	1.086	1	146.55	0.804
	126.60	1.086		147.15	0.804
2	132.45	1.058	1	157.05	0.786
	133.00	1.057		158.45	0.786
1	139.65	1.031			
	140.50	1.030			
1	.52.30	0.997			

PLATE 16

X-ray Powder Photographs

Figure 1. X-ray powder photograph of pleonaste from the Caballo Mountains. FeK_α radiation.

Figure 2. X-ray powder photograph of pleonaste from the Caballo Mountains. CuK_α radiation.

Figure 1

Figure 2

Composition and Cell Content

Table 4 below shows a quantitative chemical analysis of pleonaste and the molecular ratios of the constituents (Matthew E. Carlisle, analyst).

TABLE 4

Chemical Analysis of Pleonaste

Constituent	Percent	Ratio
Al_2O_3	65.07	0.638
MgO	17.16	0.425
FeO	17.51	0.243
Cr_2O_3	0.05	0.0003
MnO	nil	---
SnO_2	nil	---
TiO_2	nil	---
ZnO	trace	---
SiO_2	trace	---
Total	99.79	

In making the chemical analysis, 4.025 grams of the mineral was used. The highly refractory nature of pleonaste is attested to by the fact that when fused in molten sodium carbonate for 20 days, the material lost less than 1 percent by weight. Similarly, when treated with hydrofluoric acid for 20 days, the material lost less than 1 percent by weight. Solution was finally attained by fusing the pleonaste with molten potassium bisulfate for 20 days. The pleonaste was not ground before chemical analysis because the high hardness presented the possibility of contamination by grinding. The analytical procedure of Scott was followed.

The molecular ratios were determined by dividing

the percentage of each elemental oxide by its molecular weight. In recasting the chemical formula, the molecular ratios (Table 4) were placed in the general pleonaste formula. From the general formula for pleonaste, $(Fe,Mg)O\cdot Al_2O_3$, the molecular ratio between the Al_2O_3 and the sum of the FeO and the MgO would have to be equal. The amount of Cr_2O_3 is negligible. The sum of the FeO and MgO is higher by 0.30 ratio units than the Al_2O_3. All of the iron would be oxidized to the Fe_2O_3 state when fused in potassium bisulfate so that in the analysis there would be no test for FeO. The results in table 4 are based on the assumption that all the iron was in the plus 2 oxidation state. However, the above unbalance demands some Fe_2O_3 and requires the general formula for the pleonaste to be $(Fe,Mg)O\cdot(Fe,Al)_2O_3$. Recasting the chemical formula on this basis produced the following results:

Constituent	Percent	Ratio
Al_2O_3	65.07	0.638
FeO	16.07	0.224
MgO	17.16	0.425
Cr_2O_3	0.05	---
Fe_2O_3	1.60	0.010
Total	99.95	

Changing some of the FeO to Fe_2O_3 gives a larger total amount, closer to the 100 percent total, for the analysis percentages, and gives a difference of only 0.001 ratio units between the FeO-MgO and the Fe_2O_3-Al_2O_3 totals.

The formula taken from the above data would be:

$$(Fe_{.345}Mg_{.655})O \cdot (Fe_{.016}Al_{.984})_2O_3.$$

Optical Properties

The optical properties of the pleonaste, determined by immersion oils and the petrographic microscope, are: isotropic, high refringence, $n = 1.788$ to 1.789. Grains and fragments, even when as small as 8 to 10 microns in size, are a dark green, almost opaque; fragments 2 to 4 microns in size are transparent and a dull green; fragments over 50 microns appear opaque.

THEORETICAL CONSIDERATIONS

The rocks in the thesis area come under the general heading of basalt. There is a wide variation in the composition of basalt or basaltic rocks. In relation to the amount of silica they may be oversaturated, saturated, or undersaturated. The ratio of alumina to soda, potash and lime gives additional peraluminous, metaluminous, subaluminous and peralkaline types (Shand, 1947, pp. 225-245). These are but two of the numerous variations which may change the mode and naming of the rock. Basalt is generally defined as a rock which has as its essential mineral, calcic plagioclase feldspar, and as varietal, minor, or accessory minerals: olivine, augite, hornblende, feldspathoids, biotite, iron oxides, alkali feldspars, sodic plagioclase, soda-bearing pyroxenes and amphiboles, and quartz. The mafic minerals and the calcic plagioclase and other light minerals occur in approximately equal amounts (Tyrrell, p. 128; Wahlstrom, p. 294).

The order of crystallization probably depends not only on the original composition but also on the rate of cooling, which, in turn, is a function of the injection or ejection history. The exact nature of the formation of the many types of basaltic rocks from the original melt or magma is not definitely known, but a theoretical order of crystallization of the components can be formulated. The following is a theoretical history of the rocks from the

THEORETICAL CONSIDERATIONS

The rocks in the [illegible] area come under the general heading of basalt. There is a wide variation in the composition of basalt or basaltic rocks. In relation to the amount of silica they may be oversaturated, saturated, or undersaturated. The ratio of alumina to soda, potash and lime gives additional peraluminous, metaluminous, subaluminous and peralkaline types (Shand, 1947, pp. 225-245). These are but two of the numerous variations which may change the mode and naming of the rock. Basalt is generally defined as a rock which has as its essential mineral, calcic plagioclase feldspar, and as subsidiary, minor, or accessory minerals olivine, augite, hornblende, feldspathoids, biotite, iron oxides, alkali feldspars, sodic plagioclase, soda-bearing pyroxenes and amphiboles, and quartz. The mafic minerals and the calcic plagioclase and other light minerals occur in approximately equal amounts (Tyrrell, p. 128; [illegible], p. 259).

The order of crystallization probably depends not only on the original composition but also on the rate of cooling, which, in turn, is a function of the injection or ejection history. The exact nature of the formation of the many types of basaltic rocks from the original melt or magma is not definitely known, but a theoretical order of crystallization of the components can be formulated. The following is a theoretical history of the rocks from the thesis area with the theoretical and experimental data outlined in Barth (1952), Turner and Verhoogen (1951), Tyrrell (1926), Shand (1947), and Wahlstrom (1947, 1950), as a basis. A generalized idea of the order in which the common minerals crystallize from a magma is given by Bowen's (1922) reaction series:

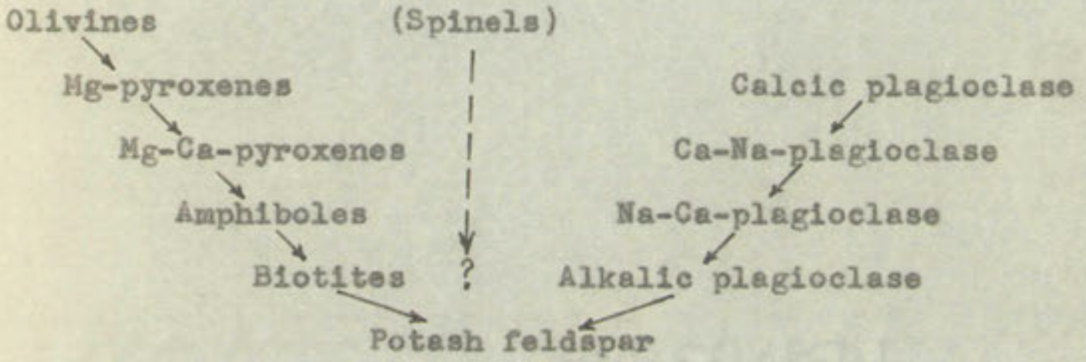

Olivine is one of the earliest minerals to crystallize in rocks, but in the presence of sufficient silica, it is converted to pyroxene (Brunton, 1952). Calcic plagioclase is also early in crystallization, slightly later than the olivine. Consider a mineral system embracing olivine (forsterite), calcic plagioclase (anorthite), and silica in a phase equilibrium diagram (Pl. 17): it is divided into five fields corresponding to the primary crystallization of silica, clinoenstatite, forsterite, anorthite and spinel. If a melt of composition a begins to crystallize, the composition of the remaining melt will change as the forsterite crystallizes, as indicated by the straight line to b where spinel would begin to crystallize. The composition would continue to change along line b-c. When

PLATE 17

Phase Equilibrium Diagram

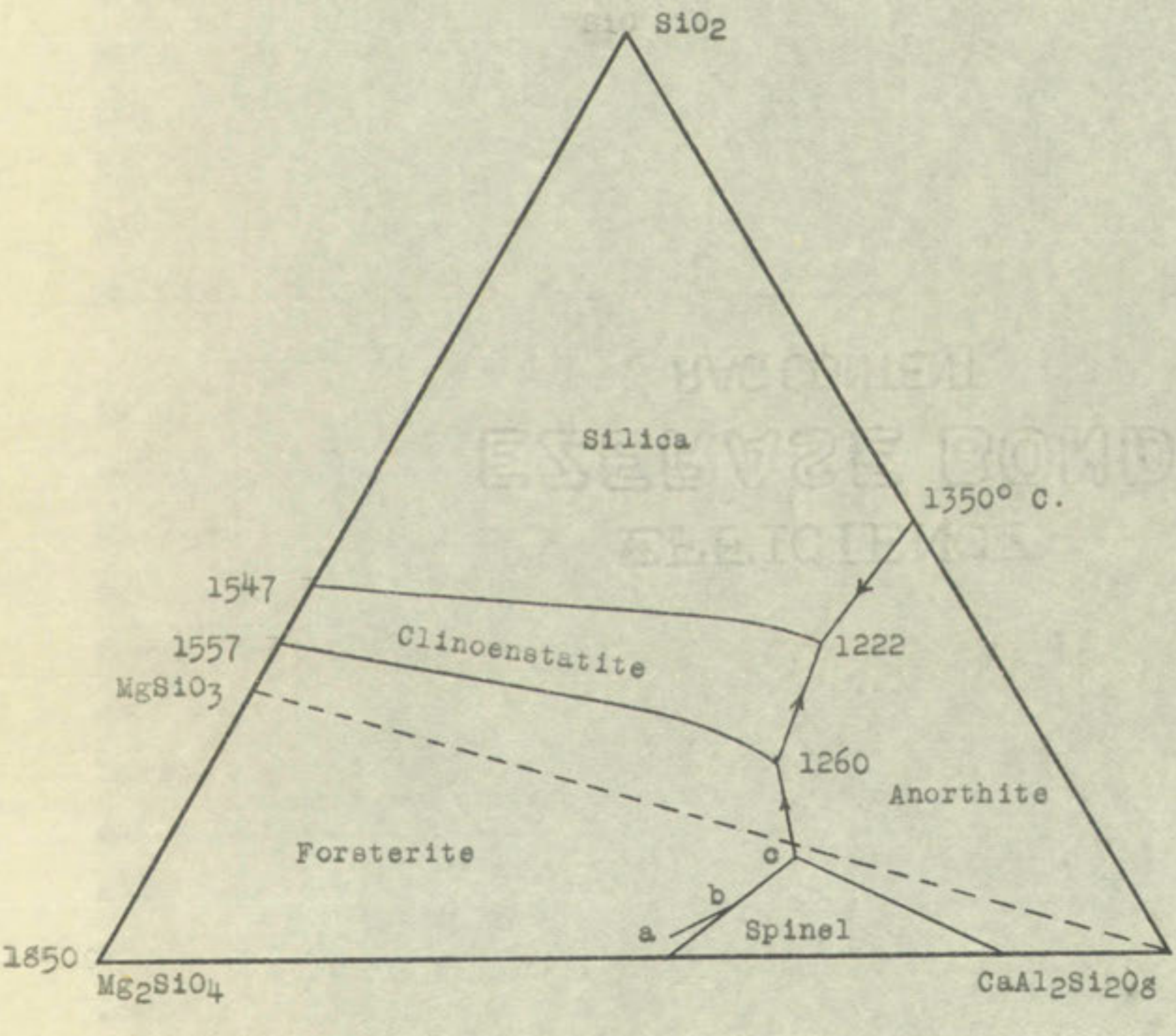

Phase diagram for the system anorthite-forsterite-silica (Turner and Verhoogen, p. 104).

point c is reached, the spinel would no longer crystallize. From point c the composition would follow along line c-1260°, with the crystallization of anorthite and forsterite. At point 1260° the forsterite would react with the liquid to form clinoenstatite. As progressive cooling takes place, the composition of the remaining liquid would follow the path of the arrows until all of the melt has crystallized. Iron in the plus 2 and plus 3 oxidation states could replace the magnesium and the aluminum to form other minerals or variations in the ones shown.

By projecting the modal composition of the rocks in the Caballo Mountains area into this diagram, a line of crystallization similar to the one outlined above would fit. Olivine and spinel could crystallize from the melt and, if the melt were high enough in the oxides of magnesium, iron, and aluminum and low enough in silica, a considerable amount of spinel and olivine could precipitate and produce large crystals. Then, with continued cooling, the olivine and spinel would be reacted upon by the liquid to produce augite and clinoenstatite. If there were s till an excess of alumina and sodium and a deficiency of silica, nepheline would crystallize in the 1404°-1490° range; if an excess of silica were present, plagioclase would form. Clinoenstatite alters readily to serpentine and would not be preserved in the rock.

The foregoing outline of events is made on the basis of continued equilibrium of the melt, but in nature

There are many disturbing elements in the order of crystallization which would preclude any possibility of the melt behaving as it theoretically should. However, an equilibrium diagram such as Plate 17 does give a good basis for the explanation of the occurrence of the various minerals in a given rock, and any inequilibrium would favor the preservation of the early-formed spinel and olivine.

CONCLUSIONS

From this study of the occurrence of large spinel crystals in a flow rock, the writer has concluded that the malt, high in the basic oxides and low in silica, was intruded in a vent or fissure, or was in the top of a magma chamber, where it remained under fairly stable conditions of temperature and pressure. This would allow the formation of large crystals of spinel and olivine, euhedral in outline, provided the conditions and composition were correct for their crystallization. The writer assumes this was true, and that the magma was then ejected and cooled rapidly enough so that very little reaction took place between the spinel and olivine crystals and the magma.

This is the first recorded occurrence of primary pleonaste in New Mexico and the first occurrence of pleonaste of such unusually large size in the Southwest. Northrop (1942) records the occurrence of "'a green magnesian spinel", or pleonaste" mentioned by Dunham (1935) as occurring in metamorphosed chert nodules in dolomite xenoliths near Goat Ranch, in a gully southeast of the Merrimac Mine, Dona Ana County, Organ district, New Mexico.

REFERENCES

Barth, Tom. F. W., 1952, Theoretical petrology: John Wiley & Sons, Inc., New York, 387 pp.

Bowen, N. L., 1922, The reaction principle in petrogenesis: Jour. Geol., vol. 30, pp. 177-198.

Brunton, G., 1952, The study of an unusual augite near Cabezon Peak, Sandoval County, New Mexico: Masters thesis, Univ. of New Mexico, 40 pp.

Buerger, M. J., 1942, X-ray crystallography: John Wiley & Sons, Inc., New York, 531 pp.

Bunn, C. W., 1949, Chemical crystallography: Clarendon Press, Oxford, 422 pp.

Clark, G. C., 1932, Applied X-rays: McGraw-Hill Book Co., Inc., New York, 470 pp.

Dana, E. S., (Revised by Wm. E. Ford) 1932, A textbook of mineralogy: John Wiley & Sons, Inc., New York, 851 pp.

Davey, W. P., 1934, A study of crystal structure and its application: McGraw-Hill Book Co., Inc., New York, 695 pp.

Dunham, K. C., 1935, The geology of the Organ Mountains, with an account of the geology and mineral resources of Dona Ana County, New Mexico: New Mexico Sch. Mines, State Bur. Mines & Min. Res., Bull. 11, 272 pp.

Kelley, V. C., and Silver, C., 1952, Geology of the Caballo Mountains: Unpublished report.

Northrop, S. A., 1942, Minerals of New Mexico: The Univ. of New Mexico Bulletin, Geol. Series, vol. 6, no. 1, 387 pp.

Phillips, F. C., 1946, An introduction to crystallography: Longmans, Green and Co., New York, 302 pp.

Scott, W. W., (Furman, N. H., Ed.) 1939, Standard methods of chemical analysis: D. van Nostrand Co., Inc., New York, 5th ed., vol. 1, 1234 pp.

Shand, S. James, 1947, Eruptive rocks: John Wiley & Sons, Inc., New York, 488 pp.

Turner, Francis J., and Verhoogen, Jean, 1951, Igneous and metamorphic petrology: McGraw-Hill Book Co., Inc., New York, 602 pp.

Tyrrell, G. W., 1926, Principles of petrology: Dutton and Co., London, 349 pp.

Wahlstrom, Ernest E., 1947, Igneous minerals and rocks: John Wiley & Sons, Inc., New York, 367 pp.

Wahlstrom, Ernest E., 1950, An introduction to theoretical igneous petrology: John Wiley & Sons, Inc., New York, 365 pp.

Winchell, Alexander N., 1951, Elements of optical mineralogy; an introduction to microscopic petrography: John Wiley & Sons, Inc., New York, 3 parts.